R-site cation randomness effect in the *A*-site ordered $Y_{0.5}La_{0.5}BaMn_2O_6$ compound*

Gao Qing-Qing(高庆庆)[a], Li Jing-Bo(李静波)[b]†, Li Guan-Nan(李冠男)[a], Rao Guang-Hui(饶光辉)[c], Luo Jun(骆 军)[a], Liu Guang-Yao(刘广耀)[a], and Liang Jing-Kui(梁敬魁)[a]

[a] *Beijing National Laboratory for Condensed Matter Physics, Institute of Physics, Chinese Academy of Sciences, Beijing* 100190, *China*
[b] *School of Materials Science and Engineering, Beijing Institute of Technology, Beijing* 100081, *China*
[c] *School of Materials Science and Engineering, Guilin University of Electronic Technology, Guilin* 541004, *China*

(Received 15 March 2013)

The *R*/Ba-ordered and *R*-site mixed compound $Y_{0.5}La_{0.5}BaMn_2O_6$ is synthesized, in which (Y, La) and Ba are regularly arranged, while Y and La randomly occupy the *R*-site. $Y_{0.5}La_{0.5}BaMn_2O_6$ has a tetragonal unit cell with a space group of *P4/mmm*. A structural transition between tetragonal and orthorhombic is observed at about 325 K by X-ray powder diffraction (XRD). Thermal magnetic measurement shows the occurrence of an antiferromagnetic transition at the temperature $T_N \sim 190$ K. Anomalies in magnetization, resistivity and lattice parameters observed around 340 K indicate a charge/orbital order transition accompanying the structural phase transition. The *R*-site randomness effect is discussed to interpret the different properties of $Y_{0.5}La_{0.5}BaMn_2O_6$ between $NdBaMn_2O_6$ and $SmBaMn_2O_6$.

Keywords: *A*-site ordering, structural transition, charge/orbital ordering, X-ray powder diffraction

PACS: 75.25.Dk, 61.50.Ks **DOI:** 10.1088/1674-1056/22/7/077502

1. Introduction

Perovskite-type manganites have been extensively studied due to their attractive physical properties as well as potential technological applications, such as colossal magnetoresistance (CMR) effect.[1,2] The intriguing physics is caused by the interplay among spin, charge, orbital, and lattice degrees of freedom.[3,4] In conventional perovskite manganite with the chemical formula $R_{1-x}A_xMnO_3$ ($R =$ rare earth elements; $A =$ Sr, Ca), *R* and *A* randomly occupy the *A* site of the structure. The electronic phase separation that results from the competition between the ferromagnetic (FM) and charge/orbital ordered (CO–OO) antiferromagnetic (AFM) components[4–6] plays a crucial role in the CMR effect of the *A*-site disordered $R_{1-x}A_xMnO_3$.[4,7] In recent years, *A*-site ordered $RBaMn_2O_6$ compounds have been successfully synthesized and extensively investigated. The electronic phase diagram is greatly modified in the *A*-site ordered $RBaMn_2O_6$,[8] compared with that of the disordered $R_{0.5}Ba_{0.5}MnO_3$. *A*-site cation ordering elevates the CO–OO transition temperature (T_{CO}) up to 380 K–480 K in the $RBaMn_2O_6$ with $R =$ Y–Sm,[9,10] as opposed to the T_{CO} of 200 K–250 K in the disordered $R_{0.5}Ca_{0.5}MnO_3$.[3,11] The charge ordering and spin ordering are even completely suppressed due to the *A*-site randomness in the $R_{0.5}Ba_{0.5}MnO_3$ for $R =$ Y–Pr.[8,12]

The *A*-site cation size effect plays an important role in the properties of *A*-site ordered $RBaMn_2O_6$ compounds. As the *R*-cation size changes, the $RBaMn_2O_6$ compounds exhibit different magnetic ground states and remarkable variations in ordering temperature.[9,10] $YBaMn_2O_6$ undergoes a CO transition at $T_{CO} \sim 480$ K and an AFM transition at $T_N \sim 190$ K,[13] whereas $LaBaMn_2O_6$ displays an FM transition at $T_C \sim 330$ K.[14,15] In the critical region around $R =$ Nd, T_C, T_N and T_{CO} almost coincide with each other, and the CO–OO phase and FM phase compete in a bicritical manner.[12,16] To investigate the role of the *A*-site cation size effect and the *R*-site randomness effect in the physical properties of $RBaMn_2O_6$, we synthesized the *R*/Ba ordered and *R*-site half doped compound $Y_{0.5}La_{0.5}BaMn_2O_6$, in which the average cation size $\langle R_{Y,La} \rangle$ is close to that of Nd^{3+}.[17] The structural and physical properties of $Y_{0.5}La_{0.5}BaMn_2O_6$ were investigated and compared with $NdBaMn_2O_6$ and $SmBaMn_2O_6$.

2. Experiments

The sample was synthesized by solid state reaction with the precursors La_2O_3, Y_2O_3 (99.99%), $Ba(NO_3)_2$ (99.0%), and MnO_2 (99.99%). The starting reagents were ground thoroughly and pressed into pellets. The pellets were sintered at 1300 °C for 30 h in flowing high-purity Ar, and then cooled to room temperature in the same atmosphere. The reductive atmosphere produced an oxygen-deficient perovskite $Y_{0.5}La_{0.5}BaMn_2O_{6-y}$. The $Y_{0.5}La_{0.5}BaMn_2O_6$ compound was obtained by annealing the $Y_{0.5}La_{0.5}BaMn_2O_{6-y}$ in flowing O_2 at 500 °C for 48 h.

The purity of the samples was checked by X-ray powder

*Project supported by the National Natural Science Foundation of China (Grant Nos. 50872148, 51072225, and 11074295) and the Natural Science Foundation of Guangxi Province, China (Grant No. 2012GXNSFGA060002).

†Corresponding author. E-mail: lijb@bit.edu.cn

© 2013 Chinese Physical Society and IOP Publishing Ltd

diffraction (XRD) using a PanAnalytical X'pert MRD high-resolution diffractometer. The XRD data used for Rietveld refinement were collected in a 2θ range from 10° to 130° with a step size of 0.017°. Temperature dependent XRD was performed in a temperature range of 15 K–400 K. The magnetic properties were studied by a superconducting quantum interference device magnetometer (MPMS 7, SQUID). Resistivity measurements were performed using the standard four-probe method by the physical property measurement system (PPMS). The microscopic structures were probed by means of transmission electron microscopy (TEM) using the JEM-2010 operating at 200 kV.

3. Results and discussion

3.1. Crystal structures

The obtained samples were identified to be single-phase by XRD. The XRD pattern of the phase was well indexed with a tetragonal space group (S.G.) of *P4/mmm*. The unit cell of the phase contains one chemical formula of $Y_{0.5}La_{0.5}BaMn_2O_6$. Rietveld refinement of the structure was performed based on the full XRD patterns using the FullProf program.[18] The refined results indicate that the Y and La ions randomly occupy the same site. The structural parameters obtained from the Rietveld refinement are listed in Table 1. $Y_{0.5}La_{0.5}BaMn_2O_6$ has a tetragonal $a_p \times a_p \times 2c_p$ unit cell, analogous to that of the reported $RBaMn_2O_6$ (R = La, Pr, and Nd),[15] where the subscript p denotes the primitive perovskite unit cell. Figure 1 shows the observed and calculated XRD patterns, and the difference profiles from Rietveld refinement.

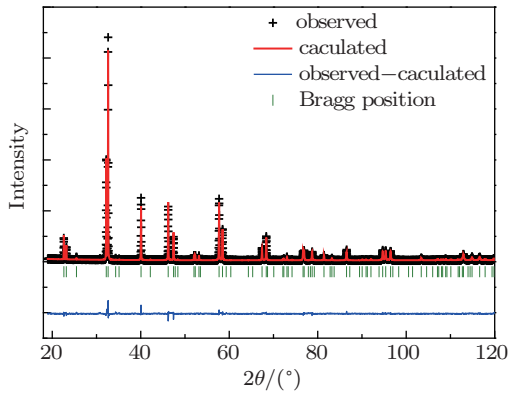


Fig. 1. (color online) Observed (cross), calculated (continuous line), and difference (bottom line) profiles obtained from Rietveld refinement of $Y_{0.5}La_{0.5}BaMn_2O_6$ at room temperature.

In the XRD pattern, the (001) reflection was too weak to be observed, while the presence of the superlattice peaks of (101), (111), (003), etc, supported the *A*-site ordering in $Y_{0.5}La_{0.5}BaMn_2O_6$. To further clarify the *A*-site ordering of $Y_{0.5}La_{0.5}BaMn_2O_6$, electron diffraction (ED) was conducted. Figure 2 shows the TEM image along the [010] zone axis; the inset gives the corresponding ED pattern. The reflections with a two-fold periodicity modulation of the primitive perovskite unit cell along the *c* axis demonstrate the *A*-site ordering.

Table 1. The refined results of $Y_{0.5}La_{0.5}BaMn_2O_6$ using tetragonal space group *P4/mmm* at room temperature; here, $a = 3.9257(4)$ Å (1 Å = 0.1 nm), $c = 7.6621(1)$ Å, $R_{wp} = 14.1\%$, and $R_e = 9.86\%$.

Atom	x	y	z	B_{iso}/Å^2
Y (La)	0.0	0.0	0.0	0.21(1)
Ba	0.0	0.0	0.5	0.21(1)
Mn	0.5	0.5	0.2463(3)	0.12(2)
O	0.5	0	0.5	1.78(6)
O	0.5	0	0.2234(6)	1.78(6)
O	0.5	0.5	0.5	1.78(6)

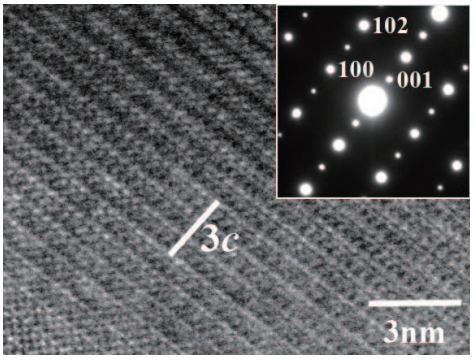


Fig. 2. The [010]-zone TEM image at room temperature. The inset shows the corresponding ED pattern.

Temperature-dependent XRD investigation was performed from 15 K to 410 K. Figure 3 shows the temperature dependence of the lattice parameters and the cell volume of the $Y_{0.5}La_{0.5}BaMn_2O_6$ compound. A structural phase transition occurs at about 325 K. Figure 4 gives the selected partial XRD patterns at 310 K and 372 K, respectively. The high-temperature (HT, $T > 325$ K) phase crystallizes in the orthorhombic symmetry with S.G. *Pmmm*. A similar structural transition was also observed in the *A*-site ordered $SmBaMn_2O_6$.[12] Figure 3 shows an abrupt change in the lattice parameters $a(b)$, c, and V at ~ 325 K. The lattice parameter $a(b)$ elongates, c contracts, and the cell volume V expands as the compound transforms from HT orthorhombic to low temperature (LT) tetragonal. This is evidence of the existence of negative expansion in the compound at ~ 325 K.

The lower symmetry of the HT phase compared with the LT modification and the negative expansion in cell volume characterize the unusual structural transition of the $Y_{0.5}La_{0.5}BaMn_2O_6$ compound. In the terminal side compound $YBaMn_2O_6$, the abnormal structural transition also exists, where the LT monoclinic phase transforms to the HT triclinic.[13] Nakajima *et al.*[13] attributed the unusual transition to the internal strain induced by the *A*-site ordering and the kinetic energy of the e_g electrons stabilized by the orbital ordering. In $Y_{0.5}La_{0.5}BaMn_2O_6$, the structural transition is accompanied by a CO–OO transition, as shown below. The

CO–OO state contributes an entropy reduction. This may partially compensate for the lattice entropy of the LT phase and make the unusual transition take place.

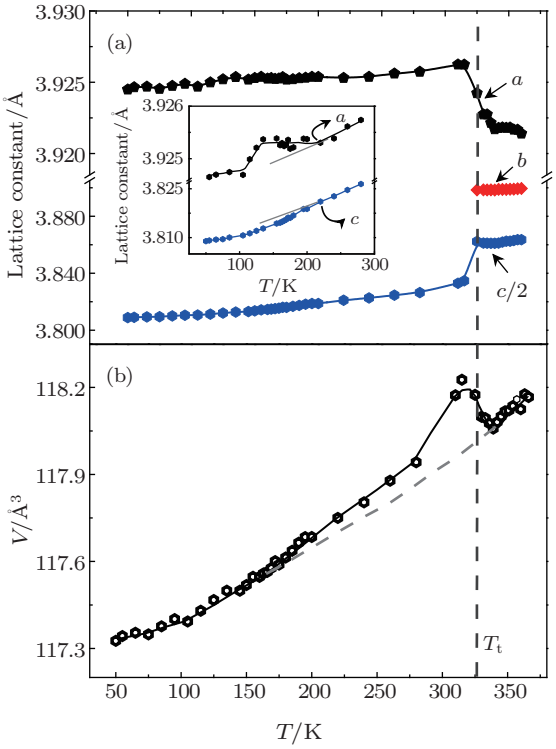


Fig. 3. (color online) The dependence of the lattice constants (a) and the cell volume (V) (b) on temperature. The inset of (a) shows the amplification of (a) around 200 K.

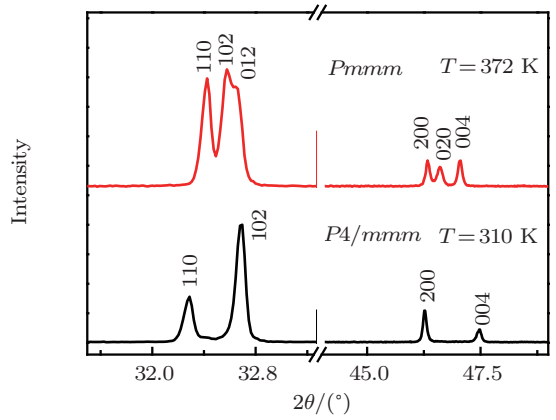


Fig. 4. (color online) The partial XRD patterns of $Y_{0.5}La_{0.5}BaMn_2O_6$ at 372 K and 310 K.

The inset of Fig. 3 shows a weak anomaly of the lattice parameters below $\sim$ 200 K. Parameter a presents a plateau, while c deviates from the linear temperature below $\sim$ 200 K. The anomaly here is consistent with the antiferromagnetic transition occurring at $\sim$ 190 K, as shown in Fig. 5.

3.2. Magnetic properties

The temperature-dependent magnetization (M–T) of the sample was measured under a magnetic field of 200 Oe (1 Oe = 79.5775 A/m) on zero-field-cooled (ZFC) and field-cooled (FC) processes, as shown in Fig. 5. The magnetization exhibits a steep reduction at $\sim$ 340 K, where the resistivity also shows an appreciable increase. Such simultaneous changes in magnetization and resistivity can be attributed to the CO–OO transition according to Ref. [19]. In the RBaMn$_2$O$_6$ (R = Tb,[20] Sm[16,20,21]) compounds, the similar behaviors of magnetization and resistivity are observed and demonstrated to result from the CO–OO transition by means of TEM, resonant X-ray scattering, and neutron diffraction techniques. As determined by XRD, the lattice parameters a (b) elongate and c shortens below $\sim$ 325 K. The changes in lattice parameters suggest that an orbital ordering with $d_{3x^2-r^2}/d_{3y^2-r^2}$ or $d_{x^2-y^2}$ type exists in the $Y_{0.5}La_{0.5}BaMn_2O_6$ compound below $\sim$ 325 K.

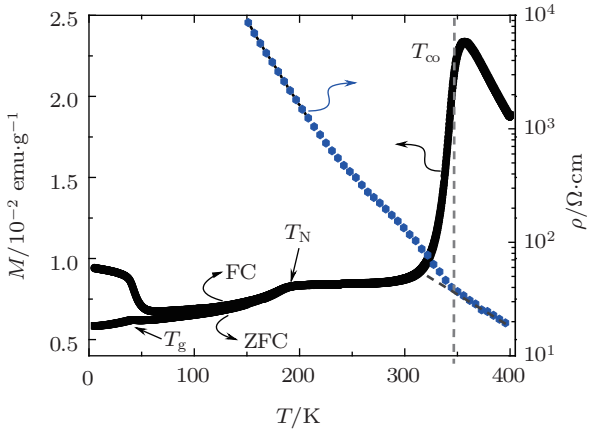


Fig. 5. (color online) Temperature-dependent electric resistivity and magnetization of the $Y_{0.5}La_{0.5}BaMn_2O_6$ sample. The magnetization is measured under a magnetic field of 200 Oe on ZFC and FC processes.

Upon further cooling, an anomaly of magnetization was observed at $\sim$ 190 K, corresponding to the antiferromagnetic transition as reported in SmBaMn$_2$O$_6$.[16,20] Below the Neel temperature, weak irreversibility of magnetizations on the FC and ZFC processes were observed, implying that some ferromagnetic components might be developed on the AFM matrix. As the temperature decreased to $\sim$ 45 K, a small cusp in the ZFC curve and a relatively large divergence between the FC and ZFC curves indicated a spin-glass-like behavior. Similar phenomena in the disordered $R_{0.5}Ba_{0.5}MnO_3$ (R = Y–Pr) were observed at $\sim$ 50 K and demonstrated to be the canonical spin-glass transition.[8,12] The spin-glass behavior in $R_{0.5}Ba_{0.5}MnO_3$ was believed to be caused by the strong uniform random potential originating from the large mismatch on the disordered A-site.[12] The spin-glass-like behavior in the present compound $Y_{0.5}La_{0.5}BaMn_2O_6$ might also be induced by disordered distributions of La and Y on the R site. Further work is required for a corroborant understanding.

Compared with RBaMn$_2$O$_6$, the R site is replaced by the mixed Y and La in $Y_{0.5}La_{0.5}BaMn_2O_6$. The average

cation size $\langle R_{Y,La}\rangle$ is close to that of Nd^{3+} but larger than Sm^{3+}.[17] However, $Y_{0.5}La_{0.5}BaMn_2O_6$ exhibits remarkably distinct phase transitions in contrast with $NdBaMn_2O_6$. In $NdBaMn_2O_6$,[15,16] no CO–OO transition was observed, and instead the strong FM correlation (not long-range FM ordering) was demonstrated to exist at $\sim$ 300 K by neutron diffraction[16], followed by an A-type AFM transition at $T_N \sim$ 275 K. The A-type AFM transition is accompanied by a uniform $d_{x^2-y^2}$ orbital ordering. While in $SmBaMn_2O_6$,[12,16] the charge/orbital ordering takes place at $\sim$ 375 K and is followed by an antiferromagnetic transition at $\sim$ 250 K.

The distinction between $Y_{0.5}La_{0.5}BaMn_2O_6$ and $NdBaMn_2O_6$ can not be explained only according to the mismatch (f) between the RO- and BaO-lattices $f = r_{R^{3+}}/r_{Ba^{2+}}$, which is an important factor related to the structure and physical properties for the single-R element $RBaMn_2O_6$.[10] For the A-site disordered compounds, another size mismatch factor σ, defined as $\sigma^2 = \sum y_i r_i^2 - \langle r_A\rangle^2$ [22,23], was usually used to interpret the lattice effect on the physical properties, where r_i, y_i, and r_A denote the ionic radius, fractional occupancy, and the average ionic radius of each A-site cation. It has been found that the increase in σ^2 reduces the FM transition temperature,[22,23] while the increase in the average A-site cation size results in a remarkable decrease in T_{CO}.[24] In present $Y_{0.5}La_{0.5}BaMn_2O_6$, the large size difference between randomly distributed Y and La on the R site results in a sufficient size mismatch $\sigma^2 \approx 0.0086$, which may lead to a distortion of the Mn–O–Mn bonds.[15,22] Consequently, the FM correlation observed in the reference compound $NdBaMn_2O_6$ is suppressed due to the large value of σ^2, and CO–OO occurs. Compared with $SmBaMn_2O_6$, the larger average cation size $\langle R_{Y,La}\rangle$ and small mismatch between the RO- and BaO-lattice play more important roles than the on-site mismatch σ^2 at R site, leading to a lower CO transition temperature in $Y_{0.5}La_{0.5}BaMn_2O_6$. Besides, the effect of σ^2 enhanced by the R-site disorder might be one reason that gives rise to the spin-glass-like behavior at $\sim$ 45 K.[8]

4. Conclusion

R/Ba ordered and R-site mixed compound $Y_{0.5}La_{0.5}BaMn_2O_6$ was synthesized by the solid-state reaction. $Y_{0.5}La_{0.5}BaMn_2O_6$ crystallizes with tetragonal symmetry (S.G.: *P4/mmm*). The structural transition between the LT tetragonal phase (*P4/mmm*) and the HT orthorhombic phase (*Pmmm*) was determined at $\sim$ 325 K by XRD, and this was accompanied by a CO–OO transition. The charge/orbital order transition at $T_{CO} \sim$ 340 K was evidenced by the steep reduction in magnetization and increase in resistivity, as well as the abrupt changes in the lattice parameters. The M–T measurements also exhibited an antiferromagnetic transition at $\sim$ 190 K and a spin-glass-like behavior at $\sim$ 45 K. The R-site cation size mismatch effect made the present $Y_{0.5}La_{0.5}BaMn_2O_6$ compound show different properties from $NdBaMn_2O_6$ and $SmBaMn_2O_6$.

References

[1] Jin S, Tiefel T H, McCormack M, Fastnacht R A, Ramesh R and Chen L H 1994 *Science* **264** 413
[2] Coey J M D, Viret M and Von Molnar S *Adv. Phys.* **48** 167
[3] Tokura Y and Nagaosa N 2000 *Science* **288** 462
[4] Dagotto E, Hotta T and Moreo A 2001 *Phys. Rep.* **344** 1
[5] Mori S, Chen C H and Cheong S W 1998 *Phys. Rev. Lett.* **81** 3972
[6] Fäth M, Freisem S, Menovsky A A, Tomioka Y, Aarts J and Mydosh J A 1999 *Science* **285** 1540
[7] Burgy J, Mayr M, Martin-Mayor V, Moreo A and Dagotto E 2001 *Phys. Rev. Lett.* **87** 277202
[8] Nakajima T, Yoshizawa H and Ueda Y 2004 *J. Phys. Soc. Jpn.* **73** 2283
[9] Nakajima T, Kageyama H, Yoshizawa H and Ueda Y 2002 *J. Phys. Soc. Jpn.* **71** 2843
[10] Ueda Y and Nakajima T 2004 *J. Phys.: Condens. Matter* **16** S573
[11] Tokunaga M, Miura N, Tomioka Y and Tokura Y 1998 *Phys. Rev. B* **57** 5259
[12] Akahoshi D, Uchida M, Tomioka Y, Arima T, Matsui Y and Tokura Y 2003 *Phys. Rev. Lett.* **90** 177203
[13] Nakajima T, Kageyama H, Ichihara M, Ohoyama K, Yoshizawa H and Ueda Y 2004 *J. Solid State Chem.* **177** 987
[14] Millange F, Caignaert V, Domengès B, Raveau B and Suard E 1998 *Chem. Mater.* **10** 1974
[15] Nakajima T, Kageyama H, Yoshizawa H, Ohoyama K and Ueda Y 2003 *J. Phys. Soc. Jpn.* **72** 3237
[16] Akahoshi D, Tomioka Y, Kubota M, Kumai R, Arima T, Matsui Y and Tokura Y 2004 *Phys. Rev. B* **70** 064418
[17] Shannon R D 1976 *Acta Crystallogr. A* **32** 751
[18] Rodriguez-Carvajal J 1993 *Physica B* **192** 55
[19] Rao C N R and Raveau B 1998 *Colossal Magnetoresistance, Charge Ordering and Related Properties of Manganese Oxides* (Singapore: World Scientific Press)
[20] Arima T, Akahoshi D, Oikawa K, Kamiyama T, Uchida M, Matsui Y and Tokura Y 2002 *Phys. Rev. B* **66** 140408
[21] García-Fernández M, Staub U, Bodenthin Y, Lawrence S, Mulders A, Buckley C, Weyeneth S, Pomjakushina E and Conder K 2008 *Phys. Rev. B* **77** 060402(R)
[22] Rodriguez-Martinez L M and Attfield J P 1996 *Phys. Rev. B* **54** R15622
[23] Attfield J P 1998 *Chem. Mater.* **10** 3239
[24] Vanitha P V, Santhosh P N, Singh R S, Rao C N R and Attfield J P 1999 *Phys. Rev. B* **59** 13539